Accepted Manuscript

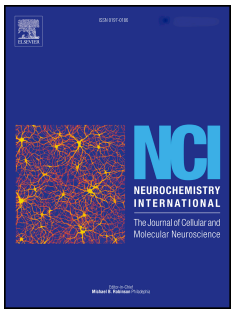

Glutathione monoethyl ester prevents TDP-43 pathology in motor neuronal NSC-34 cells

Tong Chen, Bradley J. Turner, Philip M. Beart, Lucy Sheehan-Hennessy, Chinasom Elekwachi, Hakan Muyderman

PII: S0197-0186(17)30433-3

DOI: 10.1016/j.neuint.2017.08.009

Reference: NCI 4124

To appear in: *Neurochemistry International*

Received Date: 7 August 2017

Revised Date: 0197-0186 0197-0186

Accepted Date: 11 August 2017

Please cite this article as: Chen, T., Turner, B.J., Beart, P.M., Sheehan-Hennessy, L., Elekwachi, C., Muyderman, H., Glutathione monoethyl ester prevents TDP-43 pathology in motor neuronal NSC-34 cells, *Neurochemistry International* (2017), doi: 10.1016/j.neuint.2017.08.009.

Title: Glutathione monoethyl ester prevents TDP-43 pathology in motor neuronal NSC-34 cells

Authors: Tong Chen[1], Bradley J. Turner[2], Philip M. Beart[2,3], Lucy Sheehan-Hennessy[1], Chinasom Elekwachi[1], and Hakan Muyderman[1,3]

[1]Centre for Neuroscience and Discipline of Medical Biochemistry, Flinders Medical Science and Technology, College of Medicine & Public Health, Flinders University, Adelaide, South Australia, Australia. [2]The Florey Institute of Neuroscience and Mental Health, University of Melbourne, Parkville, Victoria, Australia

[3]Corresponding authors**:**

Professor Philip Beart,
Florey Institute of Neuroscience and Mental Health,
The University of Melbourne,
Parkville,
Victoria 3010,
AUSTRALIA

E-mail address: philip.beart@florey.edu.au
Phone: 61-3-8344-7324
Fax: 61-3-9035-3107

Dr Hakan Muyderman
Discipline of Medical Biochemistry,
College of Medicine & Public Health
Flinders University,
GPO Box 2100, Adelaide,
South Australia, 5041,
AUSTRALIA

Email address: hakan.muyderman@flinders.edu.au
Phone: +61-8-8204 4221
Fax: +61-8-8374 0139

Abbreviations: Amyotrophic lateral sclerosis, ALS; TDP-43, Transactive response DNA Binding Protein 43 kDa; MN, motor neuron; GSH, glutathione; GCLM, regulatory unit of γ-glutamylcysteine ligase; GSHe, glutathione monoethyl ester; ROS, reactive oxygen species;TARDBP, TAR DNA Binding Protein; SOD, superoxide dismutase; EA, ethacrynic acid; DMEM; Dulbecco's Modified Eagle's Medium; HBSS; Hank's HEPES-buffered salt

solution; pTDP-43, phosphorylated TDP-43; SDS, sodium dodecyl sulphate; PI, propidium iodide; Eth, ethanol; GSSG, oxidised glutathione.

Abstract

Oxidative stress is recognised as central in a range of neurological diseases including Amyotrophic lateral sclerosis (ALS), a disease characterised by fast progressing death of motor neurons in the brain and spinal cord. Cellular pathology includes cytosolic protein aggregates in motor neurons and glia of which potentially cytotoxic hyper-phosphorylated fragments of the Transactive response DNA Binding Protein 43 kDa (TDP-43) constitute a major component. This is closely associated with an additional loss of nuclear TDP-43 expression indicating a "loss of function" mechanism, accelerating motor neuron (MN) loss. Furthermore, mutations in TDP-43 cause familial ALS and ALS-like disease in animal models. In this study, we investigated the role of glutathione (GSH) in modulating oxidative stress responses in TDP-43 pathology in motor neuron NSC-34 cells. Results demonstrate that depletion of GSH produces pathology similar to that of mutant TDP-43, including occurrence of cytosolic aggregates, TDP-43 phosphorylation and nuclear clearing of endogenous TDP-43. We also demonstrate that introduction of mutant TDP-43^{A315T} and silencing of endogenous TDP-43, but not overexpression of wild-type TDP-43, result in similar pathology, including depletion of intracellular GSH, possibly resulting from a decreased expression of a regulatory subunit of ɣ-glutamylcysteine ligase (GCLM), a rate limiting enzyme in GSH synthesis. Importantly, treatment of mutant cells with GSH monoethyl ester (GSHe) that directly increases intracellular GSH and bypasses the need for GSH synthesis, protected against mutant-induced TDP-43 pathology, including reducing aggregate formation, nuclear clearance, reactive oxygen species (ROS) production and cell death. Our data strongly suggest that oxidative stress is central to TDP-43 pathology and may result from a loss of function affecting GSH synthesis and that treatments directly aimed at restoring cellular GSH content may be beneficial in preventing cell death in TDP-43-mediated ALS.

Key words: Amyotrophic lateral sclerosis, TDP-43, Aggregate, Oxidative stress, Glutathione, NSC-34.

1. Introduction

Cytoplasmic accumulation of TDP-43 is a hallmark feature of many neurodegenerative disorders including Amyotrophic lateral sclerosis (ALS), a fatal neurodegenerative condition characterised by a progressive death of upper and lower motor neurons (MNs) rapidly leading to muscle paralysis and death within a few years of diagnosis (Turner et al., 2013; Kwong et al., 2007). There is no cure or effective treatment available. ALS is either familial, with a predominantly autosomal dominant inheritance pattern, or sporadic (constituting approximately 90% of all cases), with no identifiable genetic cause (Robberecht and Philips, 2013). Cellular pathology include protein aggregation, mitochondrial dysfunction, increased content of reactive oxygen species (ROS) and glutamate-mediated excitotoxicity (Rothstein 2009).

Histopathologically, a vast majority of ALS cases display cytoplasmic protein inclusions containing the protein Transactive response DNA Binding Protein 43 kDa (TDP-43), a DNA- and RNA-binding protein encoded by the TAR DNA Binding Protein (TARDBP) gene. TDP-43 is predominately localised to the nucleus where it participates in regulating transcription (Bose et al., 2008), but is also found in the cytosol where it has a regulatory role in translation and post-transcriptional modifications of pre-mRNA (Buratti and Baralle, 2008). Impaired protein processing leading to cytosolic aggregation of ubiquitinated and phosphorylated C-terminally truncated fragments of TDP-43 are cellular characteristics of TDP-43 proteinopathies (Kwong et al., 2007; Geser et al., 2008; Neumann et al., 2006). TPD-43 pathology is present in 95% of all ALS cases and in about >60% of patients with frontotemporal dementia (Neumann et al., 2007; Mackenzie, 2007).

Mutations in the TARDBP gene cause familial forms of ALS in humans and an ALS-like phenotype in transgenic animals (Gitcho et al., 2008; Kabashi et al., 2008; Rutherford et al.,

2008; Sreedharan et al., 2008; Stribl et al., 2014; Wegorzewska and Baloh, 2011). In contrast, over expression of human wild-type TDP-43 has recently been demonstrated not to result in an ALS phenotype in rodents (Mitchell *et al.* 2015).

Even in the absence of genomic mutations, TDP-43 is found in cytosolic aggregates in neurons and astrocytes, and the pathology of these cases is identical to those with a genetic background, strongly suggesting that exogenous factors induce pathogenic modifications of TDP-43. Cytosolic aggregation of TDP-43 is associated with disruption of normal cellular processes including protein degradation, response to oxidative stress and changes in mitochondrial bioenergetics (Stribl et al., 2014; Tashiro et al., 2012; Walker et al., 2013). Moreover, TDP-43 pathology is also associated with a loss of nuclear TDP-43, raising the possibility that TDP-43 pathology is mediated through a "loss of function" mechanism (Arai et al., 2006; Neumann et al., 2006). This concept is supported not only from the findings in this study but also from previous studies where silencing of TDP-43 result in cellular changes similar to those mediated by the introduction of TDP-43 mutants (Kabashi *et al.* 2010).

Oxidative damage plays a central role in cell demise in a range of neurodegenerative conditions including ALS (Muyderman and Chen, 2014). Cells with a high energy demand, such as motor neurons, constantly produce the radical superoxide as a by-product of oxidative metabolism and depend heavily on cellular processes as mediated by superoxide dismutase (SOD), catalase and glutathione (GSH)-dependent processes to minimize oxidative damage. SOD mediates the conversion of superoxide to hydrogen peroxide, which is then further detoxified by cytosolic catalase or GSH. In this context GSH directly detoxifies ROS in addition to its role as a substrate for several peroxidases (Dringen, 2000; Sims and Muyderman, 2010;Sims et al., 2004). We have previously demonstrated the importance of GSH in maintaining viability in several neural cell types, including those carrying ALS-related mutations (Muyderman et al., 2009). We have also shown that depletion of this

antioxidant directly results in mitochondrial dysfunction, ROS accumulation and cell death (Sims et al., 2004; Muyderman et al., 2007; Muyderman et al., 2004).

In ALS, experimentally decreased GSH levels enhance disease progression in transgenic $SOD1^{G93A}$ mice (Vargas et al., 2011) and loss of total GSH content has been reported in neuronal cell lines carrying the same mutation (Rizzardini et al., 2003). Moreover, decreased levels of oxidised GSH are seen in cerebrospinal fluid from ALS patients (Tohgi et al., 1999) and it was recently shown that this patient population also have reduced GSH content in motor cortex (Weiduschat et al., 2014). In addition, redox homeostasis is impaired in transgenic TDP-43 mice (Caccamo et al., 2013) and pharmacological depletion of GSH promotes cytosolic translocation of TDP-43 in cell culture models (Iguchi et al., 2013).

In the present study, we demonstrate that expression of mutant TDP-43, and the loss of endogenous TDP-43, produce disturbed production of GSH resulting in increased ROS levels and cell death which, more importantly, could be prevented by treatments that directly increases cellular GSH without the need for *de novo* synthesis.

2. Materials and Methods

2.1 Regents

All chemicals were of analytical grade and obtained from Sigma (St. Louis, MO) unless stated otherwise. Glutathione monoethyl ester (GSHe) and ethacrynic acid (EA) were purchased from Chemodex (St Gallen, Switzerland). Tissue culture reagents, propidium iodide and calcein-AM were obtained from Invitrogen (San Diego, CA). NSC-34 cells were provided by Professor Neil Cashman (University of British Columbia, Vancouver, Canada). Cell culture media and antibiotics and trypsin-EDTA were supplied by SIGMA. Fetal Bovine

Serum, N2 supplement were purchased from GIBCO (Life Technologies, San Diego), while plastic and glass culture ware was obtained from Griener (cellstar/Bio-One) purchased through SIGMA. 12mm Glass coverslips (12mm) were supplied by Thermo Fisher Scientific Inc. (Waltham, MA).

2.2 Cell cultures

Mouse NSC-34 motor neuron-like cell were grown in Dulbecco's Modified Eagle's Medium (DMEM), supplemented with 10% FBS, 1% L-glutamate and 1% mix of streptomycin and penicillin, until 80-90% confluent in a humidified atmosphere of 37°C in 5% CO_2. Media was changed every third day and cells were passaged when confluent. Cells were subcultured every 3-4 days and not used beyond passage 24. In selected experiments, differentiation was induced by the removal of serum from the culture medium and the addition of 1% N2 supplement media (DMEM, 1% FBS, 1% P/S, 1% L-glutamine and 1% N2 supplement. Differentiation was defined as the acquirement of a motor neuron-like morphology.

2.3 Transfection of NSC-34 cells

NSC-34 cells were transfected using nucleofection following the instructions from the manufacturer with minor modifications. In short, semi-confluent cultures were trypsinized (0.05% (w/v) trypsin, 0.02 % EDTA in PBS pH 7.4 for 3 min at 37°C), pelleted by centrifugation at 90 g for 10 min, re-suspended in Hank's HEPES-buffered salt solution (HBSS; in mM: 137 NaCl, 5.4 KCl, 0.41 MgSO4, 0.49 MgCl2, 1.26 CaCl2, 0.64 KH2PO4, 3.0 NaHCO3, 5.5 glucose, and 20 HEPES, pH 7.4) and counted in a haemocytometer. Cells (2.5×10^6) were mixed with 100 µl of Nucleofector solution (Nucleofector Kit V, Lonza, Cologne, Germany) and transferred to the nucleofection cuvette. Plasmid DNA was added to the mixture in a concentration of 1 µg per 10^6 cells and the cell suspension was nucleofected

using program U-029**.** Immediately after nucleofection, the cells were re-suspended in full culture medium, re-counted and plated onto poly-D-lysine and collagen coated coverslips or in poly-L-lysine coated culture plates. Culture medium was replaced 4 hours after nucleofection and every second day thereafter.

2.4 Plasmid construction

Plasmids encoding for the TDP-43^{A315T} mutation, human wild-type TDP-43 and the reporter gene mCherry only were prepared as previously described (Perera et al., 2014). Down-regulation of TDP-43 expression was performed by transfection of NSC-34 cells with a custom made miRNA generating plasmid directed at TDP-43 expression at a concentration of 2 µg/10^6 cells (BLOCK-iT™ Pol II miR RNAi Expression Vector with EmGFP under a human CMV promoter). Four constructs were made and validated by Western blot and semi-quantified against GAPDH expression. Polymerase chain reaction was used to ensure insertion of the miRNA sequence, primers used were EmGFP forward (5'GGCATGGACGA GCTGTACAA 3') and miRNA reverse (5'ACAAAGTGGGTTGATCTAGAG 3'). All plasmids were then sequenced and analysed under Vector NTI® software (Invitrogen, San Diego, USA). The construct producing the highest degree of knock-down (74 ± 6%; n=5) was used in subsequent studies. The miRNA cassette for this construct contained the following sequence: 5'TTCAGCATTGGATATATGCACGTTTTGGCCACTGACTGACGTGCATA TCCAATA3'. Control plasmid contained the reporter gene only or a non-targeting miRNA (miRNAControl, Invitrogen).

2.5 Immunocytochemistry

Immunocytochemistry was performed using antibodies directed at the full length TDP-43 (polyclonal, 1:100, Santa Cruz, CA, USA) and the normally anti-phosphorylated TDP-43-

serine 409/410 residues (pTDP-43; 1:500, Cosmos Bio, USA). Hoechst 33258 was used to visualize nuclei (1:5000, Invitrogen). In short, cells were washed in PBS and fixed for 20 min at 4˚C in 4% paraformaldehyde, washed in PBS and blocked for 30 min in PBS-BSA (1%)-Triton X-100 (0.2%). Cells were then incubated with primary antibodies overnight at 4˚C followed by washes in blocking buffer and 45 min exposure to secondary antibodies. Confocal images were captured using a Leica SP5 Spectral Confocal Microscope (Leica Microsystems, Wetzlar, Germany) and processed using ImageJ. Numbers of cells processed for image analysis were 250-350 per experiment.

2.6 Cellular fractionation

Nuclear and cytosolic fractions were produced using the Qproteome Cell Compartment Kit, (Cat#37502, QIAGEN Pty, Ltd., Hilden, Germany) following the manufacturer's instructions. Histone H3 and GAPDH were used as markers for nuclear and cytosolic fractions respectively: while nuclear fractions contained no GAPDH, cytosolic fractions contained no Histone H3 as evaluated using Western Blotting (see Fig. 5b).

2.7 Western blot

Western blot was conducted using Nupage® Novex® 4-12% Bis-Tris gel with 1.0 mm x 10 wells by Invitrogen ™ mounted on X-cell Surelock ® electrophoresis cell apparatus, and nitrocellulose membranes with 0.45mm pore size by Invitrogen, following protocols as prescribed by manufacturer. Briefly, cells were washed in PBS, lysed in sodium dodecyl sulphate **(**SDS) and then heated at 70°C for 10 min before being subjected to a 4% SDS-PAGE and transferred to a PDVF membrane. Membranes were incubated with primary antibodies against TDP-43 (1:250 Santa Cruz Biotechnologies, CA, USA), pTDP-43, (1:800, Cosmo Bio Co., LTD, Japan) and (GAPDH 1:2000, Applied Biosystems, Victoria, Australia) followed by biotinylated secondary antibody (1:3000, Vector Laboratories). Membranes were

imaged for HRP chemiluminescence using a Fujifilm LAS4000 Imager. Densitometry was performed using FujiFilm Global Multigauge (R) software. Total protein was calculated using Carestream image analysis from the total protein transferred to the blotting paper and imaged with Bio-Rad EZ Doc Gel Imager and used for normalisation.

2.8 RNA isolation and qPCR

High-quality RNA was isolated using a phenol/chloroform based method to separate RNA (Trizol) and further purification using column based isolation (RNeasy Mini Lit, Qiagen, Heiden, Germany). In short, cells were disintegrated and lysed using 1ml Trizol and a tissue lyser (Qiagen, Heiden, Germany, 3 min, 30 Hz). Chloroform (200 µl) was added to the solution, mixed for 30 s and after 3 min at room temperature centrifuged (5 min, 4°C, 12,000 rpm). The aqueous supernatant was used to isolate total RNA using a column based method including on-column DNAse digestion (RNeasy Mini Kit, Qiagen). Quantity and quality of the RNA were determined using a spectrophotometer (NanoDrop, Thermo Scientific, Australia) and a lab-on-chip system (Bioanalyzer, Agilent Technologies, Australia). Only RNA samples with RNA integrity numbers of higher than 7 were used for subsequent analysis. cDNA was synthesized using 1 µg of total RNA (iScript Reverse Transcriptase, BioRad, Australia) and used for subsequent qPCR using TaqMan and SybrGreen based qPCR. TaqMan primer assays were TDP43/Tardbp, (Mm0125750) and the reference gene Hprt (Mm01545399_m1), both Life Technologies. For SybrGreen qPCR we used mCherry, forward primer: CACTACGACGCTGAGGTCAA, reverse primer: TAGTCCTCGTTGTGGGAGGT; and the reference gene, forward primer: AGACGGCCGCATCTTCTTGTGC, reverse primer: GCCACTGCAAATGGCAGCCC. qPCR was performed using Power SYBR Green PCR master mix (Applied Biosystems) or TaqMan Gene Expression master mix (Applied Biosystems) and a StepOnePlus cycler. Relative expression levels were normalized to Hprt.

2.9 Assessing cell viability

Cell survival was assessed immediately after nucleofection using trypan blue exclusion. Cells were resuspended in HBSS, containing 0.2% trypan blue (Sigma), incubated for 5 min and counted in a haemocytometer. Blue cells were considered non-viable whereas unstained cells were considered viable. Cell viability was also assessed at 24, 48 and 72 h after nucleofection using calcein-AM or propidium iodide (PI) staining. Briefly, cells were washed in serum free culture media and incubated for 15 min at 37°C with 5% CO_2 with calcein green-AM (1 µM) or PI (25 µM). Hoechst 33258 (1:1000) was used to visualize chromatin condensation and apoptotic bodies if present. The proportion of PI positive or calcein green-AM positive cells as well as cells with apoptotic-like features (chromatin condensation, neuritic blebbing and presence of apoptotic bodies) were assessed using standard fluorescence microscopy after Hoechst 33258 staining.

2.10 Ethacrynic Acid and GSH monoethyl ester treatment

EA (70µM) or ethanol vehicle control (Eth, 1%) was prepared and diluted in culture media (final ethanol concentration <0.25%). Cells were treated in flasks or on coverslips for 5 h. GSHe was diluted directly in full culture medium to a concentration of 5 mM. Control experiments were performed with vehicle only.

2.11 Quantifying cellular GSH content

A cellular GSH assay kit supplied by Abcam (ab138881) was used to determine total, reduced and oxidised GSH. Frozen cell pellet was first thawed and suspended in Tris-EDTA lysis buffer. Following suspension in lysis buffer, cells were sonicated for 2 min in a 10 sec on/off sonication protocol. After sonication, cells were then centrifuged at 14,000 x g for 20

min and the supernatant was collected. Using a microplate reader, total, reduced and oxidized GSH measurements were calculated according to manufacturer's protocol.

2.12 Detection of Reactive Oxygen Species

To determine presence of reactive oxygen species produced by cells, a commercially available assay to detect ROS was used (Abcam - ab113851). To determine cellular ROS, 5 x 10^4 of transfected cells were plated per well in a 96-well plate and allowed to proliferate for 3 days. The assay was carried out according to manufacturer's instructions 3 days post-transfection.

2.13 Protein determination

Protein concentration assays were conducted using the DC BioRad protein assay kit (BioRad Laboratories, Hercules CA) following protocols as described by the manufacturer and absorbance read at 750 nm using a Perkin Elmer Victor ® X4 Multilabel Plate Reader.

2.13 Statistical analyses

Results are presented as mean ± SD. Each experimental condition was tested on cultures obtained from at least 3 independent passages of cells. Individual values were determined as the average of results obtained from at least three identically treated culture plates from the same experimental day and compared to control-treated sister cultures. Statistical analyses were performed on raw data by Student *t*-test or by one-way ANOVA followed by Student-Newman-Keuls test. P values <0.05 were considered significant.

3. Results

3.1 EA causes depletion of GSH in NSC-34 cells

NSC-34 cells had an average total GSH concentration of 30 ± 6 nmol/mg protein with a reduced (GSH) to oxidised glutathione (GSSG) ratio of 46 (n=5: Figure 1A). Exposure to EA (70µM, 5 h) significantly reduced total GSH content to 7.3 ± 2.8 nmol/mg which was associated with a decrease in GSH:GSSG ratio from 46 to 9 (Fig. 1A). Vehicle treatment (Eth; 1%, 5 hrs) alone did not significantly alter GSH content or the GSH: GSSG ratio (Fig. 1A). Consistent with these results, EA treatment resulted in a significant increase in cellular ROS content (Fig. 1B), but did not result in impaired cell viability at this time point (5 hr: $p>0.05$ data not shown).

3.2 EA-mediated depletion of GSH results in redistribution of endogenous nuclear TDP-43 and in the expression of pTDP-43.

While non-treated NSC-34 cells showed primarily nuclear localization of TDP-43 and low levels of pTDP-43 (Fig. 2A), the majority of EA-treated cells displayed a cytoplasmic distribution of TDP-43 associated with nuclear clearance of the protein (Fig. 2B) together with a significant increase in extra nuclear pTDP-43 immunoreactivity (Fig. 2C). To verify that EA had no direct effect on TDP-43 distribution cells were co-incubated with EA together with the cell permeable GSHe (5 mM), which counteracted EA-mediated GSH depletion (Fig. 1A), prevented increased ROS production (Fig. 1B) and cytoplasmic re-distribution and nuclear clearance of TDP-43 in these cells. GSHe was also assessed for cytotoxicity using calcein/PI as described under Methods; data demonstrated that exposure of normal NSC-34 cells to concentrations not exceeding 7.5 mM did not result in decreased cell viability (data not shown). Thus, 5 mM GSHe was used throughout the remaining study.

3.3 Transfection of NSC-34 cells

To test the impact of ALS-linked mutant TDP-43 on GSH expression, NSC-34 cells were transfected with the mCherry-tagged human TDP-43^{A315T} mutation, the human wild-type TDP-43 or with a control plasmid encoding for the reporter gene mCherry using nucleofection. This procedure resulted in transgene expression within 24 h reaching a maximum transfection efficiency of 56 ± 9%, 67 ± 11 % and 69 ± 7 % at 72 hr post-transfection, respectively (n=3). Cell death, assessed based on the ability of these cells to retain calcein fluorescence, nuclear incorporation of propidium iodide or the presence of apoptotic-like morphology changes (as described earlier), at 24, 48 or 72 h after transfection was not significantly different in cultures nucleofected with either wild-type TDP-43 or with the control plasmid compared with non-nucleofected cultures (n=5: $p>0.05$), but higher in cells expressing the TDP-43 mutant (Fig. 3). qPCR showed no significant differences in expression levels of mutant versus wild-type TDP-43 (n=3; ANOVA; $p>0.05$).3.4 Cytosolic redistribution of TDP-43 in cells expressing the A315T mutant

Transfection of NSC-34 cells with TDP-43^{A315T} resulted in cytosolic redistribution of TDP-43 in 21 ± 5 % of the cells, while cells expressing the reporter gene only showed exclusive nuclear localization of TDP-43 (Fig. 4A andB; n=5). Nuclear TDP-43 levels were also quantified using Western Blot after cellular fractionation. In cells expressing TDP-43^{A315T}, there was a significant decrease in nuclear TDP-43 expression compared to control (Fig. 5A). Control experiments verified the purity of these fractions using Histone 3 and GAPDH as markers for nuclear and cytosolic fractions respectively (figure 5b). In these cells the cytosolic fraction contained 6 ± 2 % of total TDP-43 content while the nuclear fraction contained 94 ± 5% compared to a > 65% decrease in nuclear TDP-43 content in cells carrying the mutant (Fig. 5A and B).

3.5 GSH is depleted in cells expressing the TDP-43^{A315T} mutation.

TDP-43^{A315T} expressing cells had a total GSH concentration of 5 ± 1 nmol/mg protein (n=5) representing a >80% decrease compared to the cells transfected with vector alone where then level was 24 ± 4 nmol/mg protein. Values for cells expressing wild-type TDP-43 were 28 ± 6 nmol/mg protein relative to non-transfected cells at 31 ± 3 nmol/mg protein (n=3). GSSG accounted for 15% of total GSH concentration in A315T transfected cells compared to less than 3% in non-transfected cells and in cells transfected with the control plasmids **(**Fig. 1A**)**. The GSH: GSSG ratio in A315T transfected cells was 6.25 compared to that of control transfected cells of 55. As for EA-treated cells, the introduction of the TDP-43^{A315T} mutation, but not wild-type TDP-43, resulted in significantly increased ROS levels as assessed 3 days post transfection compared to that of control cells (Fig. 1B). Depletion of GSH and increased levels of ROS content were closely associated with a decrease in cell viability in cells carrying mutant TDP-43 (Fig. 3). Furthermore, based on inconsistencies in GAPDH expression used as a loading control, we also assessed if TDP-43^{A315T} affected the expression of this key enzyme in glycolysis. Results show that there was a five-fold decrease in GAPDH expression in cells carrying the TDP-43^{A315T} mutant compared to control (Fig. 6). Hence, throughout this study, Western Blot results were normalised relative to total protein in the sample after using stain-free gels processed by Carestream image analysis and Bio-Rad EZ Doc Gel Imager.

3.6 Restoring cellular GSH content prevents TDP-43 pathology

Next, we addressed whether increasing availability of GSH in mutant TDP-43^{A315T} transfected cells reduced TDP-43 pathology. NSC-34 cells transfected with TDP-43^{A315T} or with the control vector were treated with 5 mM GSHe starting 3 h post transfection. The results demonstrated that early restoration of GSH content prevented nuclear loss of TDP-43 (Fig. 4 and 5), reducing both ROS content (Fig. 1B) and cell death (Fig. 3). Moreover, GSHe treatment also normalised GAPDH content in cells carrying the A315T mutation (Fig. 6).

Next, we investigated plausible mechanisms behind GSH depletion in cells carrying the A315T mutation by determining the expression of GSH-related proteins using Western blot. While there were no significant changes in GSH reductase or GSH peroxidase (data not shown), the results showed a several-fold decrease in the expression of the regulatory subunit of GCLM (Fig. 7) indicative of a severely impaired ability to synthesise GSH.

3.7 GSH depletion in TDP-43 pathology is mediated through a loss of function mechanism.

To establish if a loss of TDP-43 expression would result in similar disturbances to GSH homeostasis we silenced endogenous TDP-43 expression in untreated NSC-34 cells (Fig. 8). Down-regulation of TDP-43 expression was performed by transfection of NSC-34 cells with 1 µg/10^6 cells of four custom-made plasmids generating micro RNA (miRNA: 508-511) directed against TDP-43 mRNA (BLOCK-iT™ Pol II miR RNAi Expression Vector with EmGFP under a human CMV promoter). Controls were treated with a plasmid generating a non-targeting miRNA (miRNAControl, Invitrogen) and changes in TDP-43 expression were determined by immunoblotting. Silencing of TDP-43 expression using the miRNA construct with most pronounced effect resulted in an overall 50% decrease in protein expression in transfected cultures as assessed using western blot. This decrease corresponded to a near total loss of TDP-43 in individual cells expressing the construct (Fig. 8). Silencing of TDP-43 resulted in a significant decrease of GSH content (Fig. 9), several-fold increase in ROS production, and substantially increased cell death (Fig. 1B and 2)**.** However, in contrast to cells expressing the TDP-43^{A315T} mutation, cell death were not preserved in these cells after treatment with GSHe (Fig. 3), suggesting that a total depletion of TDP-43 is lethal in NSC-34 cells involving additional mechanisms in addition to ROS accumulation. Still, these data are consistent with the concept that a loss of function of TDP-43 directly results in diminished

GSH production, increased ROS production potentially leading to the aggravation of TDP-43 pathology.

4. Discussion

The present study has identified conditions under which GSH in neuronal cells expressing TDP-43^{A315T} mutant is essentially depleted, resulting in increased ROS production, TDP-43 nuclear-to-cytosolic redistribution and cell death. This study provides the first direct evidence for a critical role of cellular GSH in preserving neuronal viability in TDP-43 pathology. Loss of GSH as a result of the presence of this mutation, or in response to the depletion of endogenous TDP-43, resulted in increased intracellular ROS levels, cell death and cytosolic redistribution of TDP-43 whereas protection against mutant TDP-43-mediated cytotoxicity was provided by restoration of intracellular GSH using GSHe. Overexpression of human wild-type TDP-43 did not result in any changes in GSH content or in ROS production. This is consistent with a recent study demonstrating that exclusive overexpression of wild-type TDP-43 in transgenic mice does not result in an ALS-like phenotype (Mitchell et al., 2015).

Our results also indicated that dysregulation of TDP-43 may result from impaired expression of theGCLM, responsible for GSH synthesis, subsequent GSH depletion and increase in ROS levels. Although this evidence does not rule out other molecular mechanisms, a loss of γ-glutamylcysteine ligase activity may explain the disappointing results in previous attempts aimed at enhancing antioxidant defence processes by providing GSH precursors in ALS (Andreassen et al., 2000). Other plausible explanations include a reduction in the activity of the sodium-dependent excitatory amino acid transporter 1 that is responsible for GSH precursor uptake into these cells. This issue was not addressed in the current study but is the subject of ongoing investigations. In theory, it is also possible that cellular GSH content can be affected by release of oxidized GSH into the culture medium. This is a protective

mechanism preventing accumulation of this potentially oxidising agent (Dringen and Hirrlinger, 2003). However this was not supported by the results in the current study.

Oxidative stress, like protein aggregation, constitutes a key pathogenic mechanism of cell death in ALS. In support of this standpoint, post-mortem analyses consistently demonstrate oxidative damage and markers of oxidative damage are increased in plasma, urine and CSF of ALS patients (Muyderman and Chen, 2014; D'Amico et al., 2013). In addition, experimentally increased oxidative stress load accelerates disease progress in animal models of ALS (D'Amico et al., 2013).

A majority of ALS cases (>95%) are associated with cytosolic inclusions containing TDP-43 and the relocation of this protein from the nuclei to the cytoplasm, changes that are likely to make a significant contribution to cellular dysfunction and subsequent pathology. In addition to changes in protein folding and degradation, cytosolic accumulation of TDP-43 causes oxidative stress and mitochondrial dysfunction (*vide supra*). Given that GSH plays a critical role in cellular defence against oxidative stress in various neurodegenerative conditions, it is surprising that its role in ALS remains poorly understood. Especially considering that redox-mediated signalling previously has been linked to the regulation of TDP-43 and that oxidative stress promotes TDP-43 cross-linking via cysteine oxidation and disulphide bond formation leading to decreased TDP-43 solubility (Cohen et al., 2012).

In this study we reproduced the finding of a previous study demonstrating that depletion of GSH results in increased cytosolic aggregation of TDP-43 (Iguchi et al., 2013) and expanded on these studies to demonstrate that the content of GSH in cells carrying mutant TDP-43 is not optimal and that restoring this antioxidant pool, using a treatment that does not require GSH synthesis, prevented pathology.

Treatment with GSHe rapidly restored intracellular GSH levels and prevented TDP-43 pathology in NSC-34 cells carrying TPD-43^{A315T}. In contrast to GSH, which is poorly transported into cells and do not pass the blood brain barrier, GSHe is cell-permeable, readily de-esterified by intracellular esterases and rapidly increases intracellular GSH content (Wadey et al., 2009; Muyderman et al., 2007) We have previously demonstrated the beneficial effects of GSHe of increasing glutathione content in both *in vitro* and *in vivo* models (Muyderman et al., 2007; Muyderman et al., 2004). We have also shown that such treatment significantly improves cellular resistance against oxidative stress and that the depletion of this antioxidant directly correlates with increased susceptibility to oxidative damage. Moreover, pre-symptomatic administration of GSHe has recently proven somewhat beneficial in increasing lifespan in the SOD-1^{G93A}, albeit demonstrating a very modest effect of approximately 10% (Winkler et al., 2014). However, in this study, GSHe was given as a daily intraperitoneal injection and GSH levels in spinal cord or brain were not determined making it highly plausible that the major increase in cellular GSH was contained to the abdominal cavity. Nevertheless it highlights the need for anti-oxidant treatment in ALS and indicates the central role of GSH in this process. Thus, the characterization of TDP-43-mediated GSH depletion in our present study complements these data and has generated several unique insights into the properties of this key antioxidant in TDP-43 pathology. Most notably that mutant TDP-43 as well as silencing of endogenous TDP-43, depletes intracellular GSH and that its replacement provides overall cellular protection. In this context, a few previous studies also suggest that TDP-43 pathologies are associated with an imbalance in antioxidant redox buffering systems, with mitochondrial dysfunction most likely responsible for the increase in ROS production seen in GSH depleted cells (Caccamo et al., 2013; Iguchi et al., 2012). In addition, alterations of cellular redox state may lead to decreased protein clearance (Niforou et al., 2014), indicating that modifications of cellular

functions by oxidative stress may result in protein aggregation as seen in TDP-43 pathology. This evidence is in line with our current results showing that restoring cellular GSH content prevents cytosolic redistribution and nuclear clearance of TDP-43. In support of this concept, ALS cases show proteasomal impairment associated with an increase in oxidative stress markers (Ilieva et al., 2007; Kim et al., 2009; Neutzner et al., 2012; Tashiro et al., 2012) and increased ROS production is intimately associated to impairment of the removal of ubiquitinated proteins (Cohen *et al.* 2012). Moreover, experimentally decreased GSH accelerates disease progression in the $SOD1^{G93A}$ transgenic (Vargas et al., 2011) and loss of total GSH content in motor neurons has been reported in cell lines carrying the same mutation (Rizzardini et al., 2003).Additionally, reduced levels of GSSG have been reported in cerebrospinal fluid from ALS patients (Tohgi et al., 1999) and we have recently shown a reduction in mitochondrial GSH in $mSOD1^{G93A}$ expressing NSC-34 cells (Muyderman et al., 2009).

In addressing the mechanisms underlying the reduction in cellular GSH, we observed a several-fold decrease in the regulatory subunit of the rate limiting enzyme responsible for GSH synthesis in cells expressing mutant $TDP\text{-}43^{A315T}$. This result is most likely the major reason for the observed depletion of cellular GSH and increase in ROS content in these cells and is supported from previous studies in which genetic deletion of GCLM resulted in decreased GSH content and increased susceptibility to oxidative stress (Botta et al., 2008; Mohar et al., 2009).

Finally we demonstrated that silencing of endogenous TDP-43 produced similar changes to those produced by the introduction of mutant TDP-43 in regard to GSH depletion and cellular ROS content. This finding implies additionally that TDP-43 pathology, at least to some extent, is mediated through a “loss of action” mechanism consistent with previous studies showing that transgenic mice with a partial loss of TDP-43 function show progressive

neurodegeneration with a phenotype similar to those of animal models of ALS (Yang et al., 2014). In contrast to cells expressing mutant TDP-43, GSHe treatment did not salvage cells depleted of TDP-43. This is not surprising as a total loss of TDP-43 function would result in severe cellular dysfunction in which GSH depletion and ROS accumulation would constitute minor effects. However, the results highlight the role of TDP-43 in redox regulation and GSH synthesis.

In summary, this study demonstrates that normal TDP-43 function may be regulated via redox mechanisms and that oxidative stress is central to TDP-43 proteinopathy, most likely dependent on impaired synthesis of GSH. We propose that a loss of TDP-43 function leads to the depletion of GSH and thereby further aggravates pathological cytosolic protein aggregation and impairment of cell function. Together, our data strongly indicate that treatments directly aimed at restoring intracellular GSH will attenuate formation of cytosolic TDP-43 aggregates and reduce MN death in TDP-43-mediated ALS. Thus, intra-CSF administration of such restorative agents would constitute a feasible approach to increase MN viability and slow disease progression if translated to human subjects.

Acknowledgements: This work was supported by the National Health and Medical Research Council (NHRC, Australia: APP1023780). PMB was supported by a NRMRC Fellowship (APP1020401). Dr Turner was partly funded by the Stafford Fox Medical Research Foundation and the Florey Institute of Neuroscience and Mental Health receives infrastructure support from the Victorian State Government (Australia).

References

Andreassen O. A., Dedeoglu A., Klivenyi P., Beal M. F. and Bush A. I., 2000. N-acetyl-L-cysteine improves survival and preserves motor performance in an animal model of familial amyotrophic lateral sclerosis. Neuroreport 11, 2491-2493.

Arai T., Hasegawa M., Akiyama H., Ikeda K., Nonaka T., Mori H., Mann D., Tsuchiya K., Yoshida M., Hashizume Y. and Oda T., 2006. TDP-43 is a component of ubiquitin-positive tau-negative inclusions in frontotemporal lobar degeneration and amyotrophic lateral sclerosis. Biochem. Biophys. Res. Commun. 351, 602-611.

Bose J. K., Wang I. F., Hung L., Tarn W. Y. and Shen C. K., 2008. TDP-43 overexpression enhances exon 7 inclusion during the survival of motor neuron pre-mRNA splicing. J. Biol. Chem. 283, 28852-28859.

Botta D., White C. C., Vliet-Gregg P., Mohar I., Shi S., McGrath M. B., McConnachie L. A. and Kavanagh T. J., 2008. Modulating GSH synthesis using glutamate cysteine ligase transgenic and gene-targeted mice. Drug Metab Rev. 40, 465-477.

Buratti E. and Baralle F. E., 2008. Multiple roles of TDP-43 in gene expression, splicing regulation, and human disease. Front Biosci. 13, 867-878.

Caccamo A., Medina D. X. and Oddo S., 2013. Glucocorticoids exacerbate cognitive deficits in TDP-25 transgenic mice via a glutathione-mediated mechanism: implications for aging, stress and TDP-43 proteinopathies. J. Neurosci. 33, 906-913.

Cohen T. J., Hwang A. W., Unger T., Trojanowski J. Q. and Lee V. M., 2012. Redox signalling directly regulates TDP-43 via cysteine oxidation and disulphide cross-linking. EMBO J. 31, 1241-1252.

D'Amico E., Factor-Litvak P., Santella R. M. and Mitsumoto H., 2013. Clinical perspective on oxidative stress in sporadic amyotrophic lateral sclerosis. Free Radic. Biol. Med. 65, 509-527.

Dringen R., 2000. Metabolism and functions of glutathione in brain. Prog. Neurobiol. 62, 649-671.

Dringen R. and Hirrlinger J., 2003. Glutathione pathways in the brain. Biol. Chem. 384, 505-516.

Geser F., Winton M. J., Kwong L. K., Xu Y., Xie S. X., Igaz L. M., Garruto R. M., Perl D. P., Galasko D., Lee V. M. and Trojanowski J. Q., 2008. Pathological TDP-43 in parkinsonism-dementia complex and amyotrophic lateral sclerosis of Guam. Acta Neuropathol. 115, 133-145.

Gitcho M. A., Baloh R. H., Chakraverty S., Mayo K., Norton J. B., Levitch D., Hatanpaa K. J., White C. L., III, Bigio E. H., Caselli R., Baker M., Al-Lozi M. T., Morris J. C., Pestronk A., Rademakers R., Goate A. M. and Cairns N. J., 2008. TDP-43 A315T mutation in familial motor neuron disease. Ann. Neurol. 63, 535-538.

Iguchi Y., Katsuno M., Niwa J., Takagi S., Ishigaki S., Ikenaka K., Kawai K., Watanabe H., Yamanaka K., Takahashi R., Misawa H., Sasaki S., Tanaka F. and Sobue G., 2013. Loss of TDP-43 causes age-dependent progressive motor neuron degeneration. Brain 136, 1371-1382.

Iguchi Y., Katsuno M., Takagi S., Ishigaki S., Niwa J., Hasegawa M., Tanaka F. and Sobue G., 2012. Oxidative stress induced by glutathione depletion reproduces pathological modifications of TDP-43 linked to TDP-43 proteinopathies. Neurobiol. Dis. 45, 862-870.

Ilieva E. V., Ayala V., Jove M., Dalfo E., Cacabelos D., Povedano M., Bellmunt M. J., Ferrer I., Pamplona R. and Portero-Otin M., 2007. Oxidative and endoplasmic reticulum stress interplay in sporadic amyotrophic lateral sclerosis. Brain 130, 3111-3123.

Kabashi E., Lin L., Tradewell M. L., Dion P. A., Bercier V., Bourgouin P., Rochefort D., Bel H. S., Durham H. D., Vande V. C., Rouleau G. A. and Drapeau P., 2010. Gain and loss of function of ALS-related mutations of TARDBP (TDP-43) cause motor deficits in vivo. Hum. Mol. Genet. 19, 671-683.

Kabashi E., Valdmanis P. N., Dion P., Spiegelman D., McConkey B. J., Vande V. C., Bouchard J. P., Lacomblez L., Pochigaeva K., Salachas F., Pradat P. F., Camu W., Meininger V., Dupre N. and Rouleau G. A., 2008. TARDBP mutations in individuals with sporadic and familial amyotrophic lateral sclerosis. Nat. Genet. 40, 572-574.

Kim S. H., Shi Y., Hanson K. A., Williams L. M., Sakasai R., Bowler M. J. and Tibbetts R. S., 2009. Potentiation of amyotrophic lateral sclerosis (ALS)-associated TDP-43 aggregation by the proteasome-targeting factor, ubiquilin 1. J. Biol. Chem. 284, 8083-8092.

Kwong L. K., Neumann M., Sampathu D. M., Lee V. M. and Trojanowski J. Q., 2007. TDP-43 proteinopathy: the neuropathology underlying major forms of sporadic and familial frontotemporal lobar degeneration and motor neuron disease. Acta Neuropathol. 114, 63-70.

Mackenzie I. R., 2007. The neuropathology of FTD associated With ALS. Alzheimer Dis. Assoc. Disord. 21, S44-S49.

Mitchell J. C., Constable R., So E., Vance C., Scotter E., Glover L., Hortobagyi T., Arnold E. S., Ling S. C., McAlonis M., Da C. S., Polymenidou M., Tessarolo L., Cleveland D. W. and Shaw C. E., 2015. Wild type human TDP-43 potentiates ALS-linked mutant TDP-43 driven progressive motor and cortical neuron degeneration with pathological features of ALS. Acta Neuropathol. Commun. 3, 36.

Mohar I., Botta D., White C. C., McConnachie L. A. and Kavanagh T. J., 2009. Glutamate cysteine ligase (GCL) transgenic and gene-targeted mice for controlling glutathione synthesis. Curr. Protoc. Toxicol. Chapter 6, Unit6.

Muyderman H. and Chen T., 2014. Mitochondrial dysfunction in amyotrophic lateral sclerosis - a valid pharmacological target? Br. J. Pharmacol. 171, 2191-2205.

Muyderman H., Hutson P. G., Matusica D., Rogers M. L. and Rush R. A., 2009. The human G93A-superoxide dismutase-1 mutation, mitochondrial glutathione and apoptotic cell death. Neurochem. Res. 34, 1847-1856.

Muyderman H., Nilsson M. and Sims N. R., 2004. Highly selective and prolonged depletion of mitochondrial glutathione in astrocytes markedly increases sensitivity to peroxynitrite. J. Neurosci. 24, 8019-8028.

Muyderman H., Wadey A. L., Nilsson M. and Sims N. R., 2007. Mitochondrial glutathione protects against cell death induced by oxidative and nitrative stress in astrocytes. J. Neurochem. 102, 1369-1382.

Neumann M., Kwong L. K., Sampathu D. M., Trojanowski J. Q. and Lee V. M., 2007. TDP-43 proteinopathy in frontotemporal lobar degeneration and amyotrophic lateral sclerosis: protein misfolding diseases without amyloidosis. Arch. Neurol. 64, 1388-1394.

Neumann M., Sampathu D. M., Kwong L. K., Truax A. C., Micsenyi M. C., Chou T. T., Bruce J., Schuck T., Grossman M., Clark C. M., McCluskey L. F., Miller B. L., Masliah E., Mackenzie I. R., Feldman H., Feiden W., Kretzschmar H. A., Trojanowski J. Q. and Lee V. M., 2006. Ubiquitinated TDP-43 in frontotemporal lobar degeneration and amyotrophic lateral sclerosis. Science 314, 130-133.

Neutzner A., Li S., Xu S. and Karbowski M., 2012. The ubiquitin/proteasome system-dependent control of mitochondrial steps in apoptosis. Semin. Cell Dev. Biol. 23, 499-508.

Niforou K., Cheimonidou C. and Trougakos I. P., 2014. Molecular chaperones and proteostasis regulation during redox imbalance. Redox. Biol. 2, 323-332.

Perera N. D., Sheean R. K., Scott J. W., Kemp B. E., Horne M. K. and Turner B. J., 2014. Mutant TDP-43 deregulates AMPK activation by PP2A in ALS models. PLoS. One. 9, e95549.

Rizzardini M., Lupi M., Bernasconi S., Mangolini A. and Cantoni L., 2003. Mitochondrial dysfunction and death in motor neurons exposed to the glutathione-depleting agent ethacrynic acid. J. Neurol. Sci. 207, 51-58.

Robberecht W. and Philips T., 2013. The changing scene of amyotrophic lateral sclerosis. Nat. Rev. Neurosci. 14, 248-264.

Rothstein J. D., 2009. Current hypotheses for the underlying biology of amyotrophic lateral sclerosis. Ann. Neurol. 65 Suppl 1, S3-S9.

Rutherford N. J., Zhang Y. J., Baker M., Gass J. M., Finch N. A., Xu Y. F., Stewart H., Kelley B. J., Kuntz K., Crook R. J., Sreedharan J., Vance C., Sorenson E., Lippa C., Bigio E. H., Geschwind D. H., Knopman D. S., Mitsumoto H., Petersen R. C., Cashman N. R., Hutton M., Shaw C. E., Boylan K. B., Boeve B., Graff-Radford N. R., Wszolek Z. K., Caselli R. J., Dickson D. W., Mackenzie I. R., Petrucelli L. and Rademakers R., 2008. Novel mutations in TARDBP (TDP-43) in patients with familial amyotrophic lateral sclerosis. PLoS. Genet. 4, e1000193.

Sims N. R. and Muyderman H., 2010. Mitochondria, oxidative metabolism and cell death in stroke. Biochim. Biophys. Acta 1802, 80-91.

Sims N. R., Nilsson M. and Muyderman H., 2004. Mitochondrial glutathione: a modulator of brain cell death. J. Bioenerg. Biomembr. 36, 329-333.

Sreedharan J., Blair I. P., Tripathi V. B., Hu X., Vance C., Rogelj B., Ackerley S., Durnall J. C., Williams K. L., Buratti E., Baralle F., de B. J., Mitchell J. D., Leigh P. N., Al-Chalabi A., Miller C. C., Nicholson G. and Shaw C. E., 2008. TDP-43 mutations in familial and sporadic amyotrophic lateral sclerosis. Science 319, 1668-1672.

Stribl C., Samara A., Trumbach D., Peis R., Neumann M., Fuchs H., Gailus-Durner V., Hrabe de A. M., Rathkolb B., Wolf E., Beckers J., Horsch M., Neff F., Kremmer E., Koob S., Reichert A. S., Hans W., Rozman J., Klingenspor M., Aichler M., Walch A. K., Becker L., Klopstock T., Glasl L., Holter S. M., Wurst W. and Floss T., 2014. Mitochondrial dysfunction and decrease in body weight of a transgenic knock-in mouse model for TDP-43. J. Biol. Chem. 289, 10769-10784.

Tashiro Y., Urushitani M., Inoue H., Koike M., Uchiyama Y., Komatsu M., Tanaka K., Yamazaki M., Abe M., Misawa H., Sakimura K., Ito H. and Takahashi R., 2012. Motor neuron-specific disruption of proteasomes, but not autophagy, replicates amyotrophic lateral sclerosis. J. Biol. Chem. 287, 42984-42994.

Tohgi H., Abe T., Yamazaki K., Murata T., Ishizaki E. and Isobe C., 1999. Increase in oxidized NO products and reduction in oxidized glutathione in cerebrospinal fluid from patients with sporadic form of amyotrophic lateral sclerosis. Neurosci. Lett. 260, 204-206.

Turner M. R., Hardiman O., Benatar M., Brooks B. R., Chio A., de C. M., Ince P. G., Lin C., Miller R. G., Mitsumoto H., Nicholson G., Ravits J., Shaw P. J., Swash M., Talbot K., Traynor B. J., Van den Berg L. H., Veldink J. H., Vucic S. and Kiernan M. C., 2013. Controversies and priorities in amyotrophic lateral sclerosis. Lancet Neurol. 12, 310-322.

Vargas M. R., Johnson D. A. and Johnson J. A., 2011. Decreased glutathione accelerates neurological deficit and mitochondrial pathology in familial ALS-linked hSOD1(G93A) mice model. Neurobiol. Dis. 43, 543-551.

Wadey A. L., Muyderman H., Kwek P. T. and Sims N.R., 2009. Mitochondrial glutathione uptake: characterization in isolated brain mitochondria and astrocytes in culture. J. Neurochem. 109 Suppl 1, 101-108.

Walker A. K., Soo K. Y., Sundaramoorthy V., Parakh S., Ma Y., Farg M. A., Wallace R. H., Crouch P. J., Turner B. J., Horne M. K. and Atkin J. D., 2013. ALS-associated TDP-43 induces endoplasmic reticulum stress, which drives cytoplasmic TDP-43 accumulation and stress granule formation. PLoS. One. 8, e81170.

Wegorzewska I. and Baloh R. H., 2011. TDP-43-based animal models of neurodegeneration: new insights into ALS pathology and pathophysiology. Neurodegener. Dis. 8, 262-274.

Weiduschat N., Mao X., Hupf J., Armstrong N., Kang G., Lange D. J., Mitsumoto H. and Shungu D. C., 2014. Motor cortex glutathione deficit in ALS measured in vivo with the J-editing technique. Neurosci. Lett. 570, 102-107.

Winkler E. A., Sengillo J. D., Sagare A. P., Zhao Z., Ma Q., Zuniga E., Wang Y., Zhong Z., Sullivan J. S., Griffin J. H., Cleveland D. W. and Zlokovic B. V., 2014. Blood-spinal cord barrier disruption contributes to early motor-neuron degeneration in ALS-model mice. Proc. Natl. Acad. Sci. U. S. A 111, E1035-E1042.

Yang C., Wang H., Qiao T., Yang B., Aliaga L., Qiu L., Tan W., Salameh J., McKenna-Yasek D. M., Smith T., Peng L., Moore M. J., Brown R. H., Jr., Cai H. and Xu Z., 2014. Partial loss of TDP-43 function causes phenotypes of amyotrophic lateral sclerosis. Proc. Natl. Acad. Sci. U. S. A 111, E1121-E1129.

Figure legends

Fig. 1. Analyses of GSH (A) and oxidative stress (B) in motor neuronal NSC-34 cells. Values are mean ± S.D. (full details in Materials and methods). **(A)** Total, reduced and oxidized (GSSG) GSH expression in NSC-34 cells after treatment with; from left to right 70 µM EA for 5 hours, EA-treated cells treated with 5 mM GSHe, 1% ethanol (Eth vehicle) cells overexpressing the human wild-type TDP-43 (Wt), cells transfected with the TDP-43^{A315T} mutation, cells transfected with the TDP-43^{A315T} mutation and treated with 5 mM GSHe for 72 h, cells transfected with a control plasmid encoding for the reporter gene mCherry only and non-treated cells (NT). *** $p<0.001$ ANOVA with SNK, n=5. **(B)** Cellular content of reactive oxygen species (ROS) in cells identically treated as in (A) with the addition of cells depleted of TDP-43 (miRNA) and the corresponding miRNA scrambled control 72 h post-transfection. *** $p< 0.001$, ANOVA with SNK, n=5.

Fig. 2. Confocal micrographs showing extra nuclear localization of TDP-43 and pTDP-43 after 5 hours of EA treatment (70 µM EA) causing GSH depletion. Left: TDP-43 and pTDP-43 immunoreactivity (green); Middle: Nuclear stain DAPI (blue); and Right: the superimposed picture. (**A)** Full length TDP-43 and pTDP-43 immunoreactivity (green) in untreated NSC-34 cells. (**B)** Full length TDP-43 expression in cells depleted of GSH after EA treatment (arrows indicate extra nuclear TDP-43 localization). (**C)** Expression of pTDP-43 in NSC-34 cells depleted of GSH after GSH depletion. Scale bars 25 µm. One out of 5 representative experiments.

Fig. 3. Cell viability in NSC-34 cells expressing TDP-43^{A315T}, the mCherry control plasmid, miRNA or the miRNA scrambled control 24, 48 and 72 h after transfection and with or without GSHe treatment. GSHe treatment (5 mM) was initiated 3h post-transfection and this concentration was maintained throughout the experiment. Values are mean ± S.D. (full

details in Materials and methods). GSHe treatment significantly reduced cell death in cells expressing the A315T mutation (***p<0.001) but not in cells depleted of TDP-43 compared to the mCherry control and mutant cells treated with GSHe (### p<0.001compared to miRNA negative control). ANOVA with SNK, n=5.

Fig. 4. Confocal micrographs showing the redistribution of TDP-43 (green) in motor neuronal NSC-34 cells expressing the A315T mutant. Nuclei were stained with DAPI and appear blue. Arrows indicate extra nuclear TDP-43 localization (n=5). (**A)**. Cytosolic redistribution of TDP-43 (green) in cells transfected with TDP-43^{A315T} (mCherry; red). (**B)** Cells expressing the reporter gene only (mCherry; red). (**C)** Normalization of TDP-43 immunoreactivity (green) in cells transfected with the A315T mutation (red) and treated with 5 mM GSHe (72h). Scale bars 25 µm.

Fig. 5. Quantitative analyses of nuclear expression of TDP-43 compared to total nuclear protein as measured after cellular fractionation and quantitative Western immunoblotting (using Carestream image analysis from the total protein transferred to the blotting paper and imaged with Bio-Rad EZ Doc Gel Imager and used for normalisation, thus no reference protein needed). Values are mean ± S.D. (**A)** NSC-34 cells transfected with the TDP-43^{A315T} mutation, cells expressing TDP-43^{A315T} and treated with GSHe, and cells transfected with the reporter gene only (Cherry) or non-transfected cells (NT). Insert: Corresponding gel image. p19-22 refers to passage number of the NSC-34 cells. *** p<0.001, ANOVA with SNK posthoc test, n=6. (**B)** Typical Western blot demonstrating the purity of nuclear and cytosolic fractions using Histone 3 (H3) and GAPDH, respectively, as markers in untreated cells (left) and in cells expressing the TDP-43^{A315T} mutant.

Fig. 6. Effect of the TDP-43^{A315T} mutation on key glycolytic enzyme GAPDH. Values are mean ± S.D. (full details in Materials and methods). GAPDH expression per mg total protein

in cells transfected with the TDP-43 mutation A315T, cells expressing mutant TDP-43 and treated with GSHe, cells transfected with the reporter gene only (Cherry) and in non-transfected cells (NT). Insert: Corresponding gel image. p19-22 refers to passage number of the NSC-34 cells. *** $p<0.001$, ANOVA with SNK posthoc test, n=6.

Fig. 7. Changes in expression of GCLM. Western immunoblotting of GCLM expression in cells transfected with the TDP-43^{A315T} mutation compared to cells transfected with the control plasmid only. Values are mean ± S.D. (full details in Materials and methods). Insert: corresponding gel image. p19-22 refers to passage number of the NSC-34 cells. *** $p<0.0001$, Student *t*-test, n=6.

Fig. 8. TDP-expression after silencing using miRNA constructs (508-511). Values are mean ± S.D. (full details in Materials and methods). TDP-43 expression relative to protein content, *** $p<0.001$, ANOVA with SNK posthoc test, n=5. Insert: corresponding gel image. Results are typical for one out of five experiments.

Fig. 9. GSH content and endogenous TDP-43 expression. Total cellular GSH content after miRNA-mediated silencing of TDP-43 expression. Values are mean ± S.D. (full details in Materials and methods).*** $p<0.001$, ANOVA with SNK posthoc test, n=3.

Figure 5 A

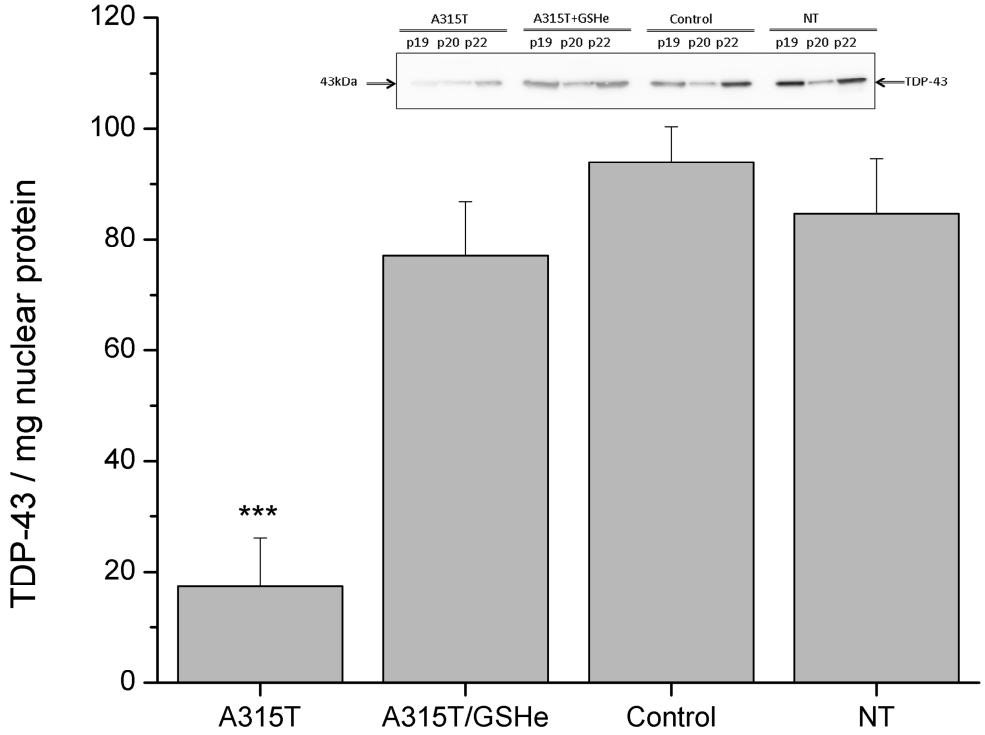

Figure 6

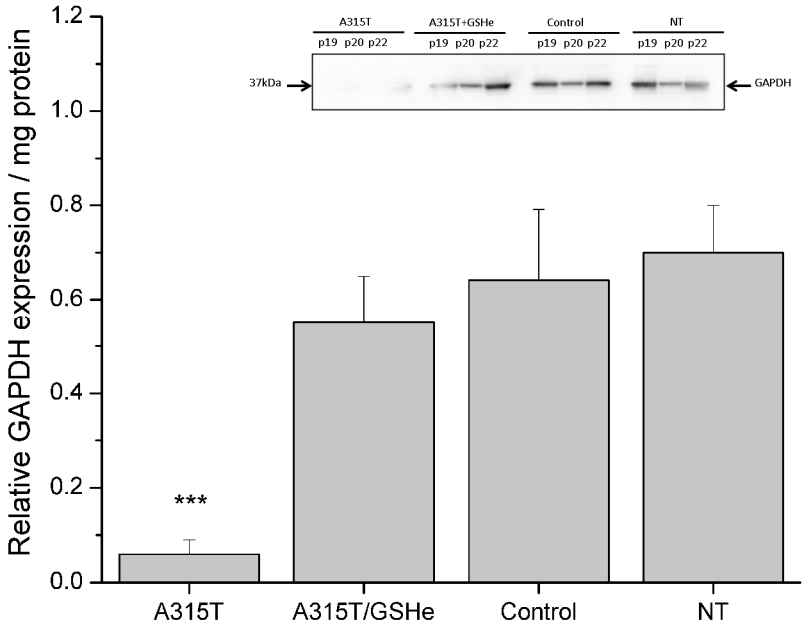

Figure 7

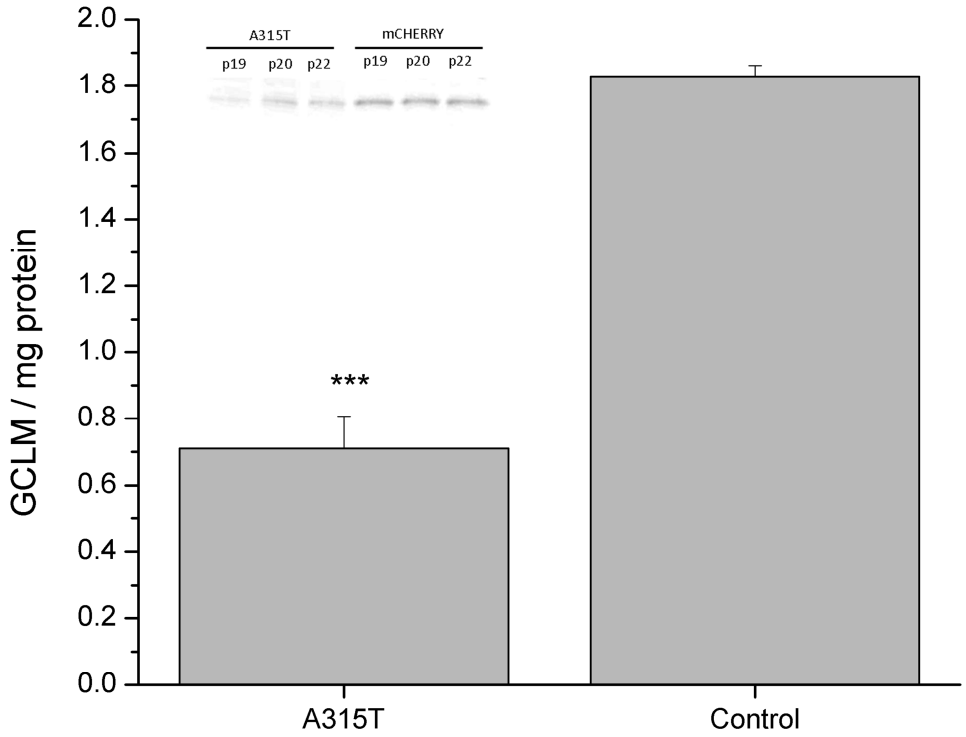

Figure 8

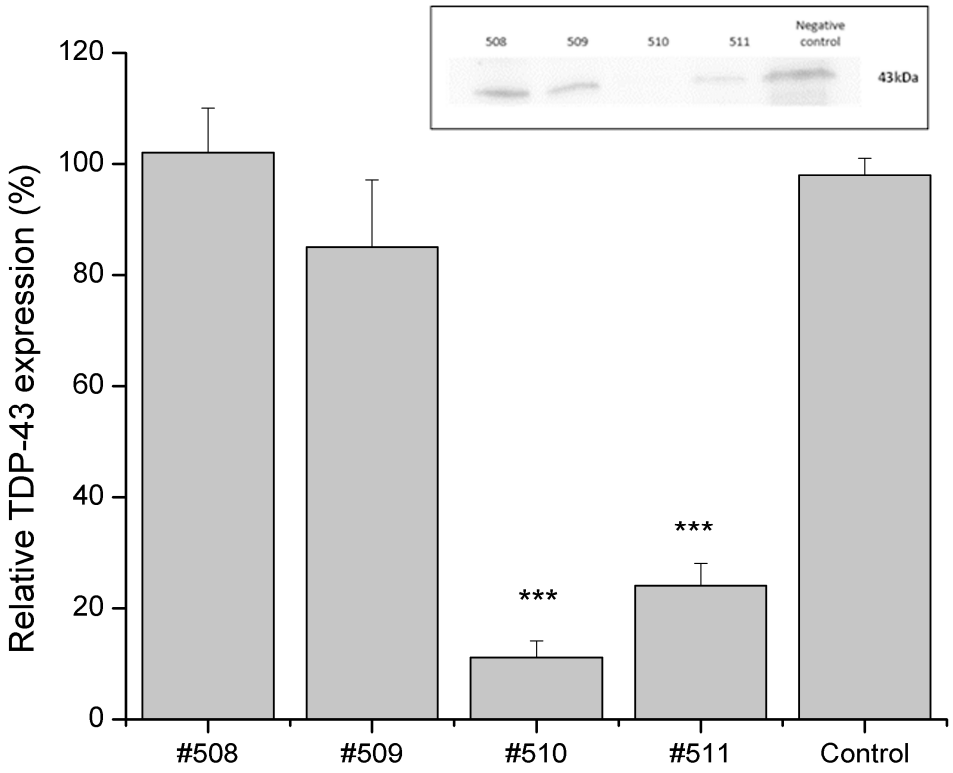

Figure 9

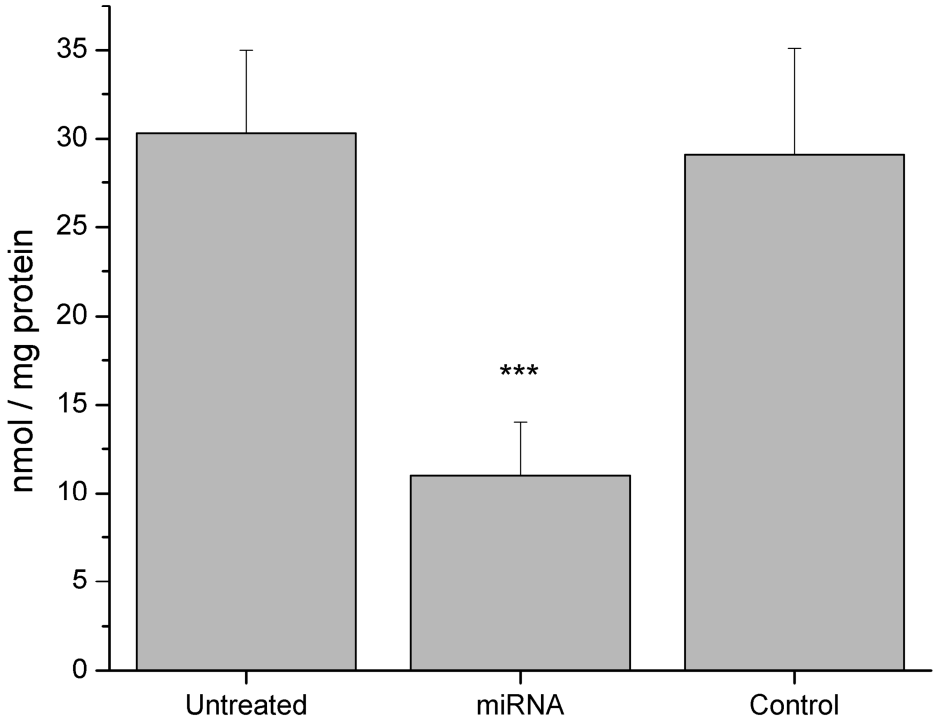

Figure 1

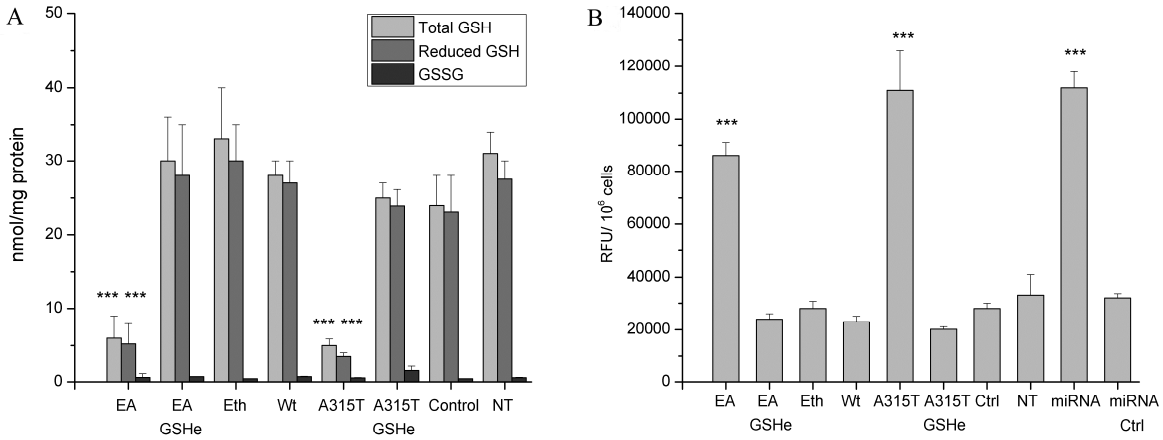

Figure 2

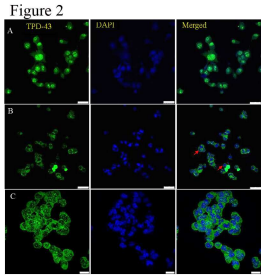

Figure 3

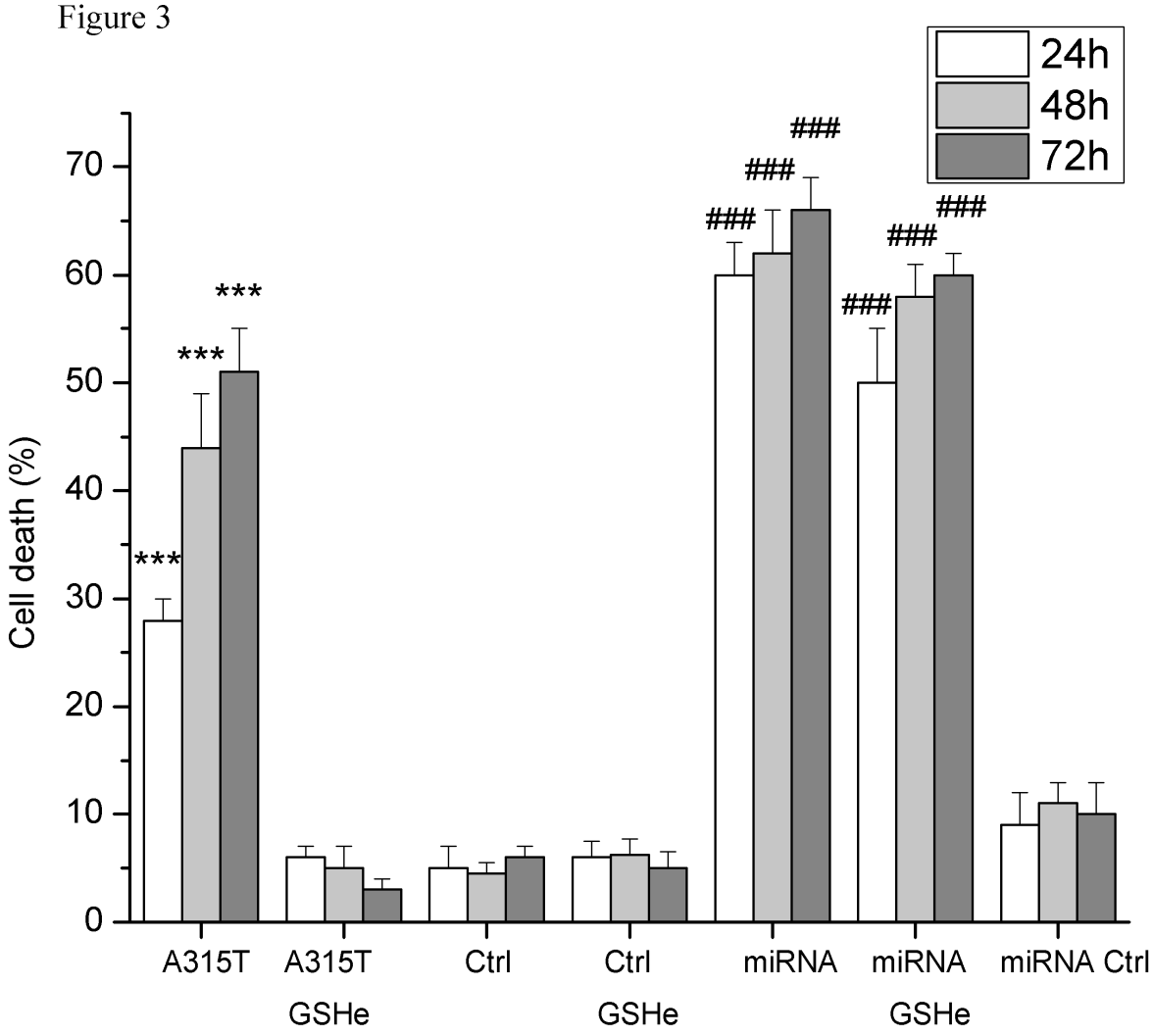

Figure 4

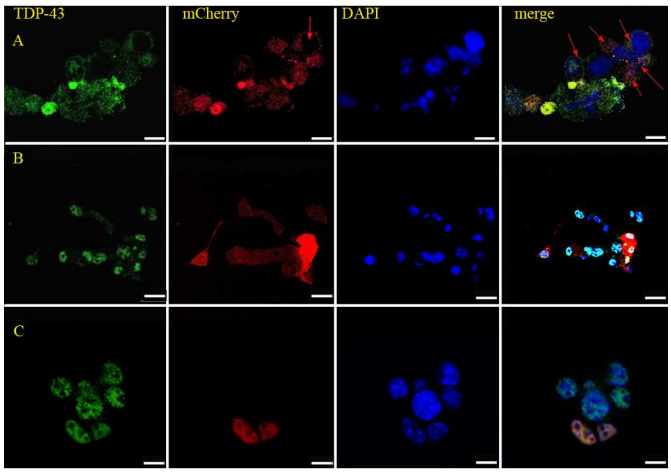

Figure 5b

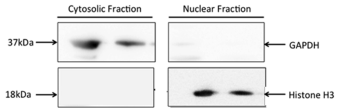

Highlights

- MND causing mutations in the TDP-43 gene result in non-functioning glutathione producing enzymes
- TDP-43/MND-causing mutations cause glutathione depletion
- Preventing, or restoring, glutathione content prevent cell death in motor neuronal NSC-34 cells expressing TDP-43 mutations causing motor neuron disease